THE JOURNAL OF BIOLOGICAL CHEMISTRY VOL. 286, NO. 9, pp. 6902–6910, March 4, 2011

Obligate Role for Ketone Body Oxidation in Neonatal Metabolic Homeostasis*[S]

Received for publication, October 7, 2010, and in revised form, November 28, 2010 Published, JBC Papers in Press, January 5, 2011, DOI 10.1074/jbc.M110.192369

David G. Cotter[‡1], **D. André d'Avignon**[§1], **Anna E. Wentz**[‡], **Mary L. Weber**[‡], **and Peter A. Crawford**[‡2]

From the Departments of [‡]*Medicine and* [§]*Chemistry, Washington University School of Medicine , St. Louis, Missouri 63110*

To compensate for the energetic deficit elicited by reduced carbohydrate intake, mammals convert energy stored in ketone bodies to high energy phosphates. Ketone bodies provide fuel particularly to brain, heart, and skeletal muscle in states that include starvation, adherence to low carbohydrate diets, and the neonatal period. Here, we use novel *Oxct1*$^{-/-}$ mice, which lack the ketolytic enzyme succinyl-CoA:3-oxo-acid CoA-transferase (SCOT), to demonstrate that ketone body oxidation is required for postnatal survival in mice. Although *Oxct1*$^{-/-}$ mice exhibit normal prenatal development, all develop ketoacidosis, hypoglycemia, and reduced plasma lactate concentrations within the first 48 h of birth. *In vivo* oxidation of ^{13}C-labeled β-hydroxybutyrate in neonatal *Oxct1*$^{-/-}$ mice, measured using NMR, reveals intact oxidation to acetoacetate but no contribution of ketone bodies to the tricarboxylic acid cycle. Accumulation of acetoacetate yields a markedly reduced β-hydroxybutyrate:acetoacetate ratio of 1:3, compared with 3:1 in *Oxct1*$^{+}$ littermates. Frequent exogenous glucose administration to actively suckling *Oxct1*$^{-/-}$ mice delayed, but could not prevent, lethality. Brains of newborn SCOT-deficient mice demonstrate evidence of adaptive energy acquisition, with increased phosphorylation of AMP-activated protein kinase α, increased autophagy, and 2.4-fold increased *in vivo* oxidative metabolism of [^{13}C]glucose. Furthermore, [^{13}C]lactate oxidation is increased 1.7-fold in skeletal muscle of *Oxct1*$^{-/-}$ mice but not in brain. These results indicate the critical metabolic roles of ketone bodies in neonatal metabolism and suggest that distinct tissues exhibit specific metabolic responses to loss of ketone body oxidation.

Transition from the intrauterine to the extrauterine environment incurs a marked shift in nutrient delivery and energy metabolism. A continuous pipeline replete with glucose and lactate, but calorically reduced in lipid, is replaced by a reduced carbohydrate, high fat milk diet that is cyclically interrupted by periods of nutrient deprivation (1–3). High energy-requiring organs like heart and skeletal muscle are poised to meet the energetic demands of this new nutrient environment because they are endowed with enzymatic machinery that avidly generates high energy phosphates from oxidative metabolism of fatty acids and lactate (4). Unlike cardiomyocytes and skeletal myocytes, most neurons oxidize fatty acids poorly and therefore remain dependent on hepatic gluconeogenesis to support energetic needs (5–8). However, because newborn brain comprises 10% of body weight and requires up to 60% of total body energy expenditure, maintenance of energetic homeostasis in the nervous system requires allocation of multiple fuels for metabolic homeostasis in the neonatal period. The rate of ketone body extraction by human neonatal brain is up to 40-fold higher than adult brain. Furthermore, ketones contribute uniquely to maturation within the nervous system (1–3, 9–16).

Most ketogenesis occurs in the liver and is driven primarily by rates of fatty acid oxidation. Mitochondrial fatty acid oxidation-derived acetoacetyl-CoA (AcAc-CoA) and acetyl-CoA together serve as the primary ketogenic substrates. Ketogenic reactions are sequentially catalyzed by HMG-CoA synthase 2 and HMG-CoA lyase, generating acetoacetate (AcAc),[3] which is converted to D-β-hydroxybutyrate (βOHB) in an NAD^+/NADH-coupled redox reaction catalyzed by βOHB dehydrogenase. AcAc and βOHB diffuse into the bloodstream and are delivered to ketolytic organs, in which they are exceptionally energy-efficient substrates (12, 17–22). Within mitochondria of ketolytic organs, βOHB is oxidized back to AcAc in a reaction catalyzed by βOHB dehydrogenase. AcAc receives a CoA moiety from succinyl-CoA, generating AcAc-CoA in a reaction catalyzed by succinyl-CoA:3-oxo-acid CoA-transferase (SCOT, EC 2.8.3.5), encoded by nuclear *Oxct1.* This enzyme is not expressed in liver (12, 23). Mitochondrial AcAc-CoA thiolase catalyzes conversion of AcAc-CoA to acetyl-CoA, which is terminally oxidized within the tricarboxylic acid cycle.

Reports of ~20 individuals who harbor homozygous or compound heterozygous *OXCT1* loss-of-function mutations (Online Mendelian Inheritance in Man 245050) indicate that a functional allele is required for ketone body oxidation, and as such patients typically present in infancy with spontaneous ketoacidosis (24–31). Numerous single-nucleotide polymorphisms have been identified within the human *OXCT1* locus, but functional significance has been ascribed to relatively few of them.

Adverse consequences of ketoacidosis are well appreciated, and physiological states that increase ketone body turnover have been extensively analyzed. Nonetheless, experimental models to date

* This work was supported, in whole or in part, by National Institutes of Health Grants DK020579 and DK073282. This work was also supported by a pilot and feasibility grant from the Diabetic Cardiovascular Disease Center at Washington University.

[S] The on-line version of this article (available at http://www.jbc.org) contains supplemental Table S1 and Fig. S1.

[1] Both authors contributed equally to this study.

[2] To whom correspondence should be addressed: Dept. of Medicine, Washington University School of Medicine, Campus Box 8086, 660 S. Euclid Ave., St. Louis, MO 63110. Tel.: 314-747-3009; Fax: 314-362-0186; E-mail: pcrawford@wustl.edu.

[3] The abbreviations used are: AcAc, acetoacetate; AMPKα, AMP-activated protein kinase α; βOHB, D-β-hydroxybutyrate; E, embryonic day; LC3, light chain 3; P, postnatal day; SCOT, succinyl-CoA:3-oxo-acid CoA-transferase.

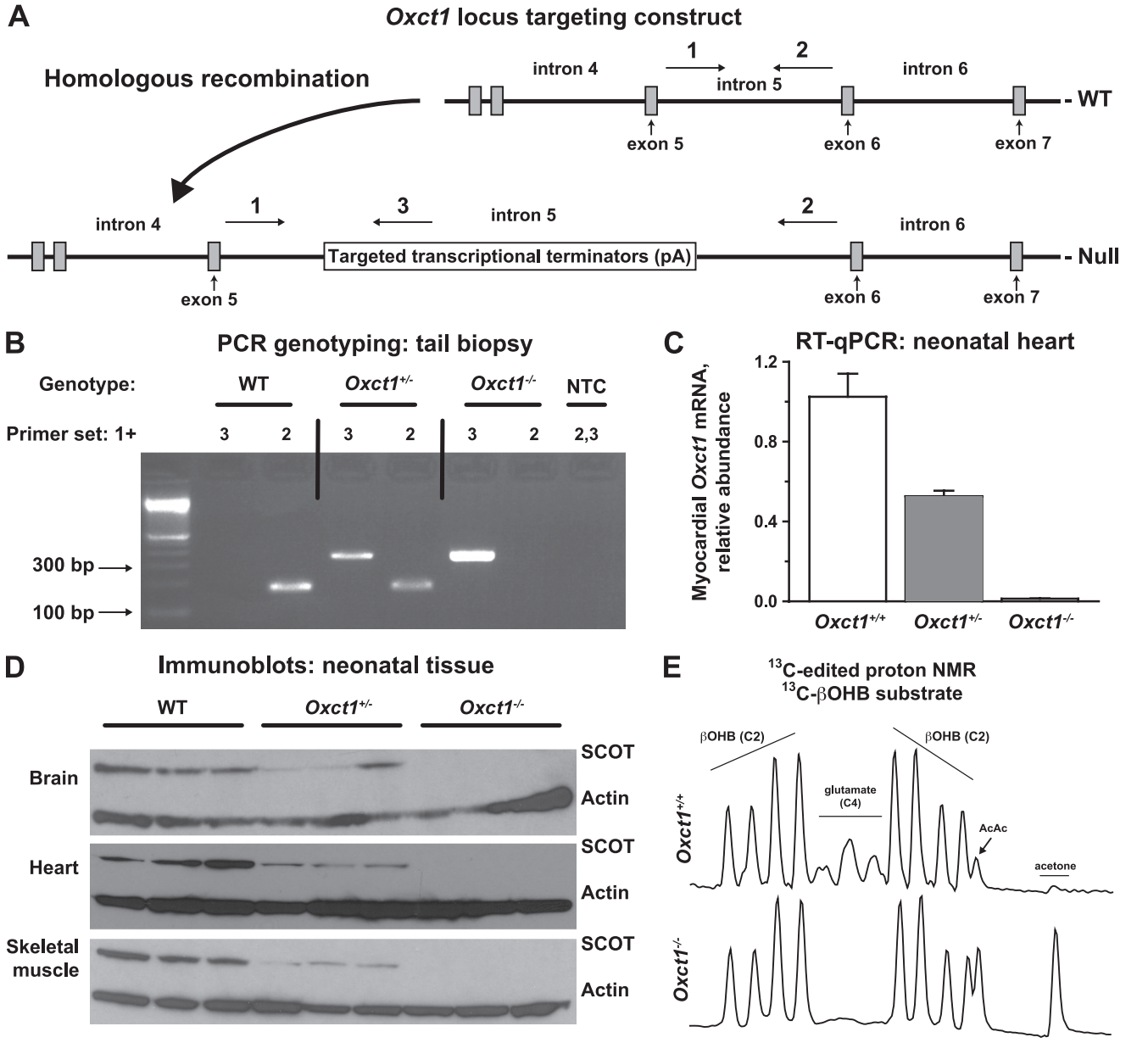

FIGURE 1. **Ketolysis-deficient *Oxct1*$^{-/-}$ mice.** *A*, targeting strategy for the *Oxct1* locus in ES cells. *WT*, wild-type locus; *Null*, loss-of-function allele. *Arrows* indicate locations of genotyping PCR primers. See supplemental Table S1 for a list of primer sequences. *B*, PCR genotyping of *Oxct1*$^{-/-}$ P0 mice. *NTC*, no template control. *C*, expression of *Oxct1* mRNA in heart of P0 *Oxct1*$^{+/+}$, *Oxct1*$^{+/-}$, and *Oxct1*$^{-/-}$ mice, determined by RT-quantitative PCR; $n = 5$/group. *D*, immunoblot of SCOT and actin using protein lysates from brain, heart, and quadriceps/hamstrings skeletal muscle of P0 *Oxct1*$^{+/+}$, *Oxct1*$^{+/-}$, and *Oxct1*$^{-/-}$ mice. *E*, ^{13}C-edited proton NMR spectrum (2.1–2.5 ppm, relative to chemical shift of trimethylsilyl propionate internal standard) from quadriceps/hamstrings of P0 *Oxct1*$^{+/+}$ and *Oxct1*$^{-/-}$ mice that had been injected with [2,4-$^{13}C_2$]βOHB 30 min prior to collection of tissues and generation of extracts. [^{13}C]Glutamate is a reporter of tricarboxylic acid flux of a ^{13}C-labeled substrate that is selectively absent in extracts from *Oxct1*$^{-/-}$ mice. *C2* and *C4* correspond to carbon position.

have not definitively revealed whether loss of ketone oxidation can be energetically tolerated, particularly at the tissue level, and the metabolic adaptations to ketolytic insufficiency are unknown. In this study, we use novel *Oxct1*$^{-/-}$ mice to examine the metabolic roles of ketone body oxidation in the neonatal period and the adaptations to its absence.

EXPERIMENTAL PROCEDURES

Animals—Oxct1$^{+/-}$ C57BL/6 mouse embryonic stem (ES) cells (clone EPD0082-1-CO2) were acquired through the National Institutes of Health knock-out mouse project (KOMP) consortium. The targeting sequence inserts two transcriptional terminators (pA) within intron 5 of the *Oxct1* locus, which is upstream from sequence that encodes critical catalytic SCOT residues (Fig. 1*A*) (32, 33). Genotyping was performed using primer sets schematized in Fig. 1*A* and listed in supplemental Table S1. ES cells were microinjected into embryonic day 3.5 (E3.5) C57BL/6 blastocysts, and four chimeric mice (determined by tail biopsy PCR) were obtained. Transmission of the targeted allele was achieved by breeding chimeric males to C57BL/6 wild-type females. Heterozygote (*Oxct1*$^{+/-}$) progeny were then crossed to generate *Oxct1*$^{-/-}$ mice. All mice were maintained on standard polysaccharide-rich chow diet (Lab Diet 5053) and autoclaved water *ad libitum*. Lights were off between 1800 and 0600. All P0 litters were obtained at 0900,

TABLE 1

Plasma metabolite concentrations in P0–P1 mice

TG, triglycerides; FFA, free (nonesterified) fatty acids; $n = 6$–10/group; **, $p < 0.01$ compared with +/−; †, $p < 0.01$ compared with +/+; aa, $p < 0.01$ and *a*, $p < 0.05$ compared with the same genotype at P0. Data are presented are mean ± S.E.; comparisons are two-way ANOVA with Bonferroni post hoc testing.

Oxct1 genotype and age	Weight	βOHB	AcAc	Glucose	Insulin	FFA	Lactate	TG
	mg	*mM*	*mM*	*mg/dl*	*ng/ml*	*mM*	*mM*	*mg/dL*
+/+, P0	1,339 ± 37	0.29 ± 0.07	0.08 ± 0.02	46 ± 19	0.47 ± 0.09	0.28 ± 0.09	1.09 ± 0.11	72.5 ± 20.6
+/−, P0	1,285 ± 28	0.50 ± 0.12	0.17 ± 0.06	49 ± 10	0.53 ± 0.16	0.24 ± 0.04	1.11 ± 0.06	72.4 ± 11.0
−/−, P0	1,301 ± 29	1.40 ± 0.36**,†	3.10 ± 1.07**,†	38 ± 11	0.30 ± 0.01	0.28 ± 0.05	1.10±.07	82.0 ± 19.0
+/+, P1	1,384 ± 60	0.66 ± 0.04	0.06 ± 0.1	65 ± 7	0.38 ± 0.04	0.96 ± 0.40^{aa}	1.36 ± 0.20	80.7 ± 16.0
+/−, P1	1,435 ± 36	0.67 ± 0.09	0.20 ± 0.06	56 ± 4	0.62 ± 0.16	0.77 ± 0.14^{a}	1.50 ± 0.11	74.8 ± 23.4
−/−, P1	1,322 ± 36	4.39 ± 0.53^{**,†,a}	11.8 ± 0.8^{**,†,aa}	19 ± 1^{**,†,a}	0.42 ± 0.06	1.14 ± 0.30^{aa}	0.67 ± 0.04^{**,†,aa}	127.8 ± 21.6

and tissues/blood were harvested mid-morning. All experiments were performed using protocols approved by the Animal Studies Committee at Washington University.

Plasma Metabolite and Insulin Measurement—Measurements of plasma glucose, AcAc, βOHB, free fatty acids, and triglycerides were performed using biochemical assays coupled to colorimetric substrates (Wako), as described previously (34). Plasma lactate was measured using a colorimetric assay (BioVision). Blood glucose was measured in duplicate using a glucometer (Aviva). Measurement of plasma insulin was performed by ELISA (Millipore) as described previously (34).

Gene Expression Analysis—Quantification of gene expression was performed using real-time RT-quantitative PCR using the ΔΔCt approach as described, normalizing to *Rpl32*, using primer sequences listed within supplemental Table S1 (34).

Immunoblotting—Immunoblots, using protein lysates from neonatal brain, heart, and quadriceps/hamstring muscles to detect Oxct1/SCOT (rabbit anti-SCOT; Proteintech Group) were performed as described (34). Detection of phospho-AMPKα (*p*-AMPKα (Thr-172)) and total AMPKα was performed as described previously (35). Microtubule-associated protein 1 light chain 3 (LC3) was detected using rabbit polyclonal anti-LC3 (NB100-2220; Novus Biologicals) and donkey anti-rabbit IgG conjugated to horseradish peroxidase (NA9340; GE Healthcare). Band intensities were quantified densitometrically using QuantityOne software (Bio-Rad).

Measurement of in Vivo Substrate Utilization—P0 mice were injected intraperitoneally with 10 μmol of sodium [2,4-$^{13}C_2$]βOHB, [1-^{13}C]glucose, or sodium [3-^{13}C]lactate (Cambridge Isotope Laboratories) per g of body weight. Because P1 *Oxct1*$^{-/-}$ mice are hypoglycemic and hypolactatemic, ^{13}C-isotope injections were supplemented in these animals with either 20 μmol/g naturally occurring glucose, for [1-^{13}C]glucose studies, or 10 μmol/g naturally occurring lactate, for [3-^{13}C]lactate studies, to ensure tissue delivery of total and ^{13}C-labeled substrate would remain equal among genotypes. After the indicated incubation durations in minutes, neonatal mice were killed by decapitation, and tissues were rapidly freeze-clamped in liquid N_2. Neutralized perchloric acid extracts were profiled using gradient heteronuclear single-quantum correlation ^{13}C-edited proton NMR measured at 11.75 T. Quantification of integrals of carbon 2 of [^{13}C]taurine (a normalizing metabolite whose tissue concentrations were constant across conditions and which is not enriched by administration of these substrates) and [^{13}C]glutamate (carbon 4) was performed as described previously (34). Signals were collected from extracts dissolved in 300 μl of D_2O + 1 mM trimethylsilyl propionate, loaded into high precision, thin walled 5-mm tubes (Shigemi).

Statistical Analyses—Analyses were performed using GraphPad software (Prism), using tests described under "Results."

RESULTS

Ketolytic Deficiency in Oxct1$^{-/-}$ *Mice*—To determine the energetic role of ketone bodies in the neonatal period, *Oxct1*$^{-/-}$ mice were generated on the C57BL/6 genetic background (Fig. 1, *A* and *B*). Genotyping analysis of *Oxct1*$^{+/-}$ × *Oxct1*$^{+/-}$ live progeny from 12 litters examined on postnatal days 0–1 (P0–P1) indicated that progeny are born in a Mendelian ratio: 19 +/+, 40 +/−, and 25 −/− mice ($\chi^2 = 0.5$, $p = 0.78$). Body weights among +/+, +/−, and −/− mice did not vary on P0 or P1; gastric milk spots were observed with equal frequency within each genotype; and no gross anatomic or behavioral abnormalities were observed in P0–P1 *Oxct1*$^{-/-}$ mice (Table 1). As expected, *Oxct1* mRNA and SCOT protein were reduced ~50% in P0 *Oxct1*$^{+/-}$ mice and were absent in *Oxct1*$^{-/-}$ mice (Fig. 1, *C* and *D*). Independent measurements of plasma biochemical metabolites on P0 and P1 revealed marked and progressive hyperketonemia in *Oxct1*$^{-/-}$ mice, with total ketone body concentrations increasing to >16 mM in *Oxct1*$^{-/-}$ mice on P1, consistent with accumulation of unmetabolized substrate (Table 1). An abnormally increased ratio of AcAc to βOHB is also consistent with a ketolytic lesion at the reaction catalyzed by SCOT: ligation of a CoA moiety to AcAc. Measurement of *in vivo* metabolism of [^{13}C]βOHB in skeletal muscle of P0 *Oxct1*$^{-/-}$ mice, using ^{13}C-edited proton NMR of extracts acquired 30 min after labeled substrate administration, confirmed the absence of ^{13}C-enriched glutamate, a quantitative surrogate for procession of carbon through the tricarboxylic acid cycle, and accumulation of [^{13}C]acetone and [^{13}C]AcAc, products of [^{13}C]βOHB that remain unmetabolized due to the absence of SCOT (Fig. 1*E*) (34, 36). These findings were corroborated in P1 skeletal muscle and in P0 and P1 brain (supplemental Fig. S1). Taken together, these results indicate that (i) *Oxct1*$^{-/-}$ mice are ketolysis-deficient and (ii) ketone body oxidation in mice does not notably proceed through SCOT-independent pathways.

Ketoacidosis, Hypoglycemia, and Neonatal Lethality of Oxct1$^{-/-}$ *Mice*—Unlike P0–P1 progeny of *Oxct1*$^{+/-}$ × *Oxct1*$^{+/-}$ pairings, genotyping analysis of live progeny from 14 litters between P2 and P10 yielded 34 +/+, 50 +/−, and zero −/− mice ($\chi^2 = 24.7$, $p < 0.0001$). No lethality phenotype

was evident in heterozygotes ($\chi^2 = 0.92$, $p = 0.34$). In addition to hyperketonemia, hypoglycemia and reduced plasma lactate concentrations were also observed in P1, but not P0 *Oxct1*$^{-/-}$ animals. Significant differences in plasma insulin, free fatty acid, and triglyceride concentrations were not observed (Table 1). In particular, the rise in plasma free fatty acid concentrations that occurs after birth in association with suckling of high fat milk was preserved in P1 *Oxct1*$^{-/-}$ mice (37, 38).

Although P1 *Oxct1*$^{-/-}$ mice exhibit marked hyperketonemia, relatively reduced plasma glucose and plasma lactate concentrations indicate that ketolytic insufficiency also results in diminution of other circulating metabolic fuels. To determine whether suckling *Oxct1*$^{-/-}$ mice could be rescued from these metabolic abnormalities and prospective energetic deficiency, we performed metabolic resuscitation experiments using newborn progeny of *Oxct1*$^{+/-}\times$ *Oxct1*$^{+/-}$ mice. Serial subcutaneous injections of 155 mM $NaHCO_3$ ± 10% glucose were delivered to suckling neonates (50 μl every 3–6 h; seven injections were administered/24-h period). Although $NaHCO_3$ partially buffers the acidifying effects of ketone bodies, glucose provides an additional energetic substrate that stimulates insulin release, thereby inhibiting ketogenesis and prospectively curtailing ketoacidosis in suckling *Oxct1*$^{-/-}$ mice (39, 40). As expected, survival analysis revealed that control suckling *Oxct1*$^{-/-}$ mice injected with 155 mM $NaHCO_3$ alone exhibited similar survival and weight course as uninjected suckling *Oxct1*$^{-/-}$ animals, indicating that partial buffering of the acidifying effects of ketone bodies had no impact on survival (Fig. 2, $n = 20$ pups/group). On the other hand, serial administration of $NaHCO_3$ + glucose markedly improved the survival and weight trajectory of suckling *Oxct1*$^{-/-}$ mice in the first 48 h of life. However, by P3, *Oxct1*$^{-/-}$ animals maintained on the $NaHCO_3$ + glucose regimen had fallen off a normal growth curve, and all gradually died over an additional 2–3 days. No significant effects of the $NaHCO_3$ + glucose, or $NaHCO_3$ alone regimens were observed in *Oxct1*$^{+/+}$ or *Oxct1*$^{+/-}$ animals.

To determine whether the failure-to-thrive phenotype observed within $NaHCO_3$ + glucose-resuscitated *Oxct1*$^{-/-}$ animals was attributable to an insufficiency of glucose uptake, plasma glucose concentrations were measured in resuscitated animals 30 and 180 min after $NaHCO_3$ + glucose administrations in P2 *Oxct1*$^{+/+}$, *Oxct1*$^{+/-}$, and *Oxct1*$^{-/-}$ mice. In addition, because SCOT-dependent ketone body metabolism within pancreatic β cells may influence glucose-stimulated insulin secretion, we also measured plasma insulin 30 min after $NaHCO_3$ + glucose administration in these mice (41, 42). Our results indicate that postinjection glucose disposal and plasma insulin concentrations were not reduced in *Oxct1*$^{-/-}$ mice (Fig. 3, *A* and *B*). However, despite treatment with the resuscitation regimen, suckling *Oxct1*$^{-/-}$ mice still developed marked hyperketonemia (Fig. 3*C*). These results indicate that although systemic glucose uptake is intact in *Oxct1*$^{-/-}$ mice, the lethal metabolic consequences of ketolytic insufficiency in suckling mice are refractory to frequent glucose administration.

Metabolic Adaptations of Oxct1$^{-/-}$ *Mice*—To determine whether the development of hypoglycemia and reduced plasma lactate concentrations result from metabolic adaptations to the loss of ketolytic capacity, we performed a series of experiments

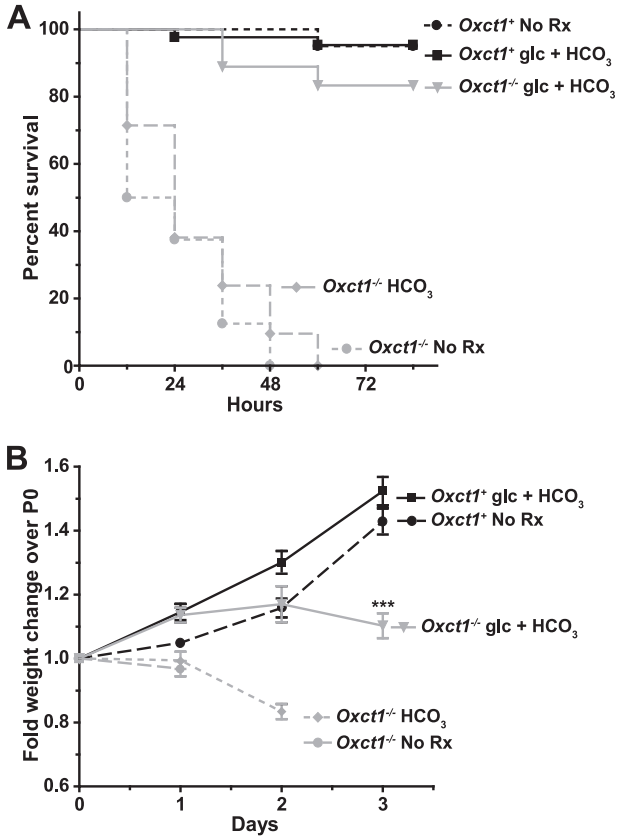

FIGURE 2. **Metabolic resuscitation of *Oxct1*$^{-/-}$ mice.** *A*, Kaplan-Meier curves for neonatal mice in the untreated, treated with 155 mM $NaHCO_3$ alone, or treated with 155 mM $NaHCO_3$ + 10% glucose (*glc*) states. Subcutaneous injections were performed every 3–6 h, starting within 3 h of birth, with seven injections over a 24-h period. *Oxct1*$^{+/+}$ and *Oxct1*$^{+/-}$ mice showed no differences and were pooled (noted as *Oxct1*$^{+}$). Within the first 90 h of life, no statistically significant differences were observed among treated *Oxct1*$^{+}$ mice, untreated *Oxct1*$^{+}$ mice, and *Oxct1*$^{-/-}$ mice treated with $NaHCO_3$ + glucose. Likewise, no statistically significant difference was observed between *Oxct1*$^{-/-}$ mice treated with $NaHCO_3$ alone and untreated *Oxct1*$^{-/-}$ mice. However, addition of glucose to the $NaHCO_3$ regimen significantly improved survival of *Oxct1*$^{-/-}$ mice in the first 90 h of life ($p < 0.001$ by log-rank test, $n = 20$/group). *B*, relative weights of animals within the genotype and treatment groups described in *A*. ***, $p < 0.001$ by two-way ANOVA with post hoc Bonferroni testing, independently compared with each of the other treatment groups.

in neonatal *Oxct1*$^{-/-}$ mice and their littermates. First, we measured the abundance of the phosphorylated (active) form of the energy sensor/effector AMPKα in skeletal muscle, heart, and brain of untreated P0 *Oxct1*$^{-/-}$ mice and their P0 *Oxct1*$^{+/+}$ littermates. To ensure that measured responses of *Oxct1*$^{-/-}$ mice were not downstream consequences of ketoacidosis and hypoglycemia, P0 mice were harvested within 3 h of birth. Protein lysates from skeletal muscle and heart of *Oxct1*$^{-/-}$ mice did not reveal evidence of AMPKα activation, but the phosphorylated form of AMPKα was augmented 6.9 ± 1.4-fold in brain of *Oxct1*$^{-/-}$ mice, suggesting tissue-specific adaptation to the absence of ketolysis ($n = 7$/group, $p < 0.01$; Fig. 4).

Second, we determined whether autophagy was altered in *Oxct1*$^{-/-}$ mice. Autophagy is an AMPK-activated self-degradative intracellular process in which organelles are recycled, prospectively in part for the purpose of energy conservation during periods of nutrient deprivation (43–45). Adaptation to

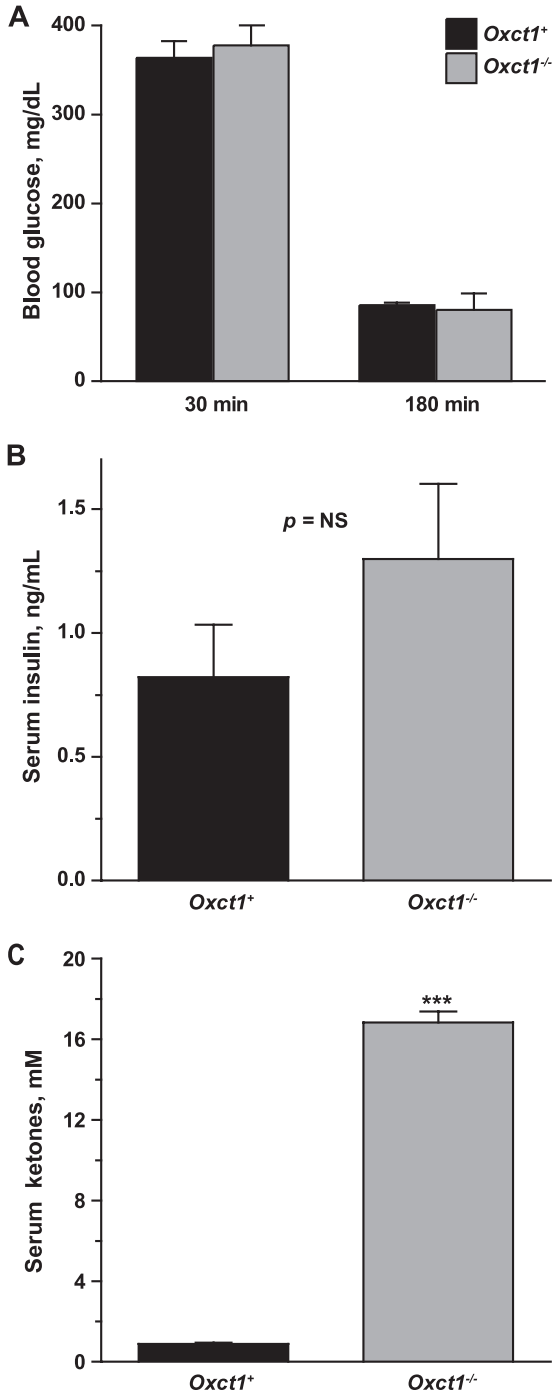

FIGURE 3. **Normal glucose disposal but refractory hyperketonemia in glucose-resuscitated suckling *Oxct1*$^{-/-}$ mice.** *A*, blood glucose concentrations measured on P2 within neonatal mice treated with the $NaHCO_3$ + glucose resuscitation regimen every 3–6 h. Measurements were taken independently 30 and 180 min after administration of $NaHCO_3$ + glucose. *B*, plasma insulin concentrations within resuscitated mice, 30 min after $NaHCO_3$ + glucose administration. *NS*, not significant. *C*, total plasma ketone concentration (βOHB + AcAc) within resuscitated mice, 30 min after $NaHCO_3$ + glucose administration. For all comparisons, *Oxct1*$^{+/+}$ and *Oxct1*$^{+/-}$ mice showed no differences and were pooled (noted as *Oxct1*$^{+}$). $n = 7$/group; ***, $p < 0.001$ by Student's *t* test.

extrauterine life requires normal autophagic progression (46). To determine whether ketolytic deficiency in brain of P0 *Oxct1*$^{-/-}$ mice is accompanied by induction of autophagy, we measured a key biomarker of autophagic progression, the differential processing/migration of protein LC3 on SDS-PAGE (47). The relative abundance of the faster migrating form of LC3 (LC3-II:LC3-I ratio) was increased 2.0 ± 0.2-fold (n = 7/group, $p < 0.001$) in brain lysates of *Oxct1*$^{-/-}$ mice (Fig. 5). This result, which was not observed in skeletal muscle (data not shown), is consistent with a proautophagic response to energy deficiency in brain of *Oxct1*$^{-/-}$ mice.

Third, to determine whether ketolytic insufficiency and the associated ultimate development of reduced plasma glucose and lactate concentrations were linked to increases in glucose and lactate utilization by tissues that normally oxidize ketones in *Oxct1*$^{-/-}$ mice, we used NMR to measure *in vivo* oxidative metabolism of independently administered [^{13}C]glucose or [^{13}C]lactate in brains and skeletal muscle of P0 and P1 *Oxct1*$^{-/-}$ mice and their littermates. Brain extracts obtained from P0 neonates 30 min after intraperitoneal administration of 10 μmol/g body weight [^{13}C]glucose revealed 2.4 ± 0.2-fold increased accumulation of ^{13}C-enriched glutamate in brains of *Oxct1*$^{-/-}$ mice compared with *Oxct1*$^{+}$ mice (from 3.6 ± 0.8% to 8.5 ± 1.7%; $n = 7$/group, $p = 0.002$; Fig. 6*A*; no differences were observed between *Oxct1*$^{+/+}$ and *Oxct1*$^{+/-}$ mice, which are combined and represented as *Oxct1*$^{+}$). As expected, at the time of tissue harvest, tissue ^{13}C enrichment of glucose (35.3% and 41.3% in *Oxct1*$^{+}$ and *Oxct1*$^{-/-}$ mice, respectively, $p = 0.51$) and total blood glucose concentrations were also equivalent between groups that received [^{13}C]glucose, indicating that increased ^{13}C enrichment of glutamate could not be explained by increased delivery of ^{13}C-substrate. These findings were corroborated in brain extracts of P0 animals collected 45 min after substrate injection: ^{13}C enrichment of glutamate was increased 2.8 ± 0.3-fold in brains of *Oxct1*$^{-/-}$ mice ($n = 5$/group, p = 0.02). Evidence for increased glucose utilization persisted in brains of *Oxct1*$^{-/-}$ mice on P1, which exhibited 1.8 ± 0.2-fold greater ^{13}C enrichment of glutamate in *Oxct1*$^{-/-}$ brains than by brains of *Oxct1*$^{+}$ littermates 30 min after substrate administration ($n = 7$/group, $p = 0.02$; Fig. 6*A*). Because P1 *Oxct1*$^{-/-}$ mice are hypoglycemic, this experiment was performed by administering a mixture of ^{13}C-labeled and naturally occurring glucose (see "Experimental Procedures"), which prevented disproportionately high delivery of labeled glucose to brains of *Oxct1*$^{-/-}$ mice. Taken together, these results are consistent with a higher rate of glucose oxidation in brains of *Oxct1*$^{-/-}$ mice on both P0 and P1, which possibly contributes to the ultimate development of hypoglycemia.

Unlike brain of *Oxct1*$^{-/-}$ mice, evidence for increased glucose oxidation was not observed in skeletal muscle, which, after 30 min of [^{13}C]glucose administration, revealed only scant ^{13}C enrichment of glutamate in *Oxct1*$^{+}$ (1.4 ± 0.2%) or *Oxct1*$^{-/-}$ mice (1.9 ± 0.3%). After 45 min, ^{13}C enrichment of glutamate increased equally to ~3% in *Oxct1*$^{+}$ and *Oxct1*$^{-/-}$ mice. Similar results were observed in muscle of P1 mice.

To obtain surrogates of *in vivo* lactate oxidation in neonatal mice, we measured [^{13}C]glutamate in brains and skeletal muscles of P0 animals 30 min after administration of 10 μmol/g [^{13}C]lactate. In *Oxct1*$^{+}$ and *Oxct1*$^{-/-}$ mice, ^{13}C labeling of glutamate in brain was greater through [^{13}C]lactate than that delivered through [^{13}C]glucose. Nonetheless, there was no difference between brains of *Oxct1*$^{+}$ and *Oxct1*$^{-/-}$ mice (11.1 ±

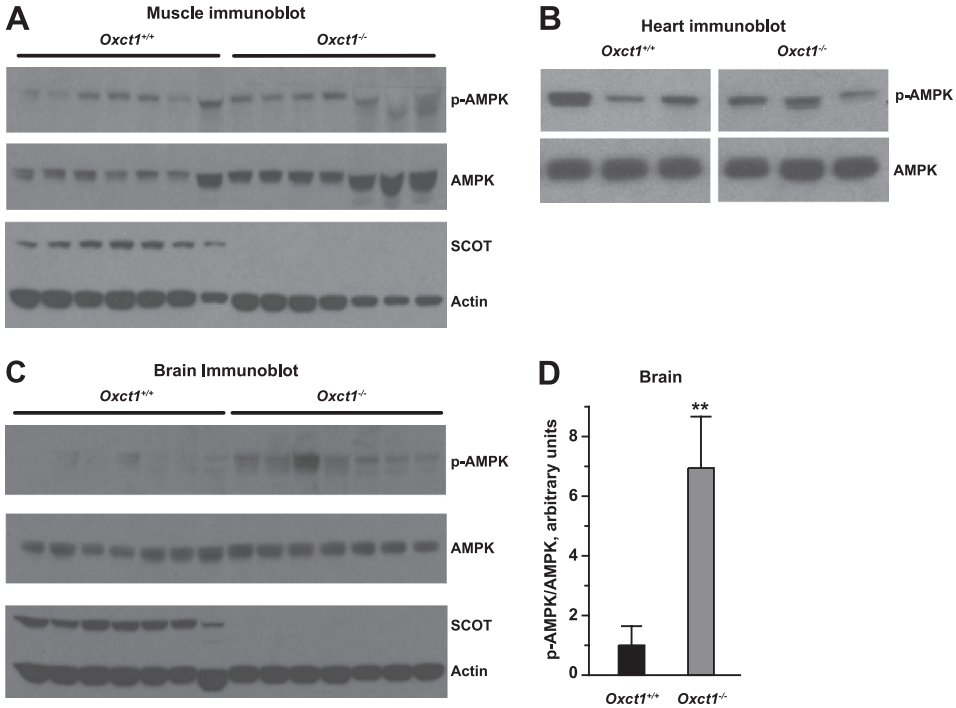

FIGURE 4. **Increased phosphorylation of AMPKα within brain of *Oxct1*$^{-/-}$ mice.** *A–C*, immunoblots of lysates from untreated animals: skeletal muscle (*A*), heart (*B*), and brain (*C*) protein lysates from P0 *Oxct1*$^{+/+}$ and *Oxct1*$^{-/-}$ mice for phospho-AMPKα (*p*-AMPKα), total AMPKα, SCOT, and actin. *D*, densitometric quantification of *p*-AMPKα:AMPKα ratio in brain lysates. **, $p < 0.01$ by Student's *t* test.

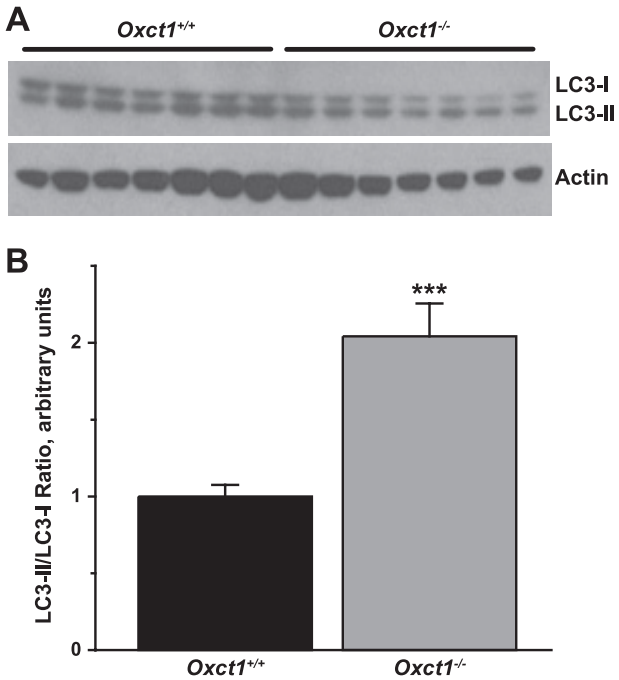

FIGURE 5. **Enhanced autophagy in brain of *Oxct1*$^{-/-}$ mice.** *A*, immunoblots of P0 brain protein lysates for LC3 and actin. *B*, densitometric quantification of LC3-II:LC3-I ratios in brain lysates. ***, $p < 0.001$ by Student's *t* test.

3.0% and 12.0 ± 3.7%, respectively, $n = 5$/group, $p = 0.84$). Conversely, ^{13}C enrichment of glutamate from lactate was enhanced in skeletal muscle of P0 *Oxct1*$^{-/-}$ mice by 1.7 ± 0.2-fold compared with skeletal muscle of *Oxct1*$^{+}$ mice (7.9 ± 0.8% and 4.5 ± 0.7%, respectively, $n = 5$/group, $p = 0.02$; Fig. 6*B*). As expected, ^{13}C enrichment of substrate was not greater in skeletal muscle of P0 *Oxct1*$^{-/-}$ mice. Increased lactate oxidation rates did not persist to P1 in skeletal muscle, which were 5.5 ± 0.4% and 5.0 ± 0.8% in P1 *Oxct1*$^{+}$ and *Oxct1*$^{-/-}$ mice, respectively ($n = 5$/group, $p = 0.6$; Fig. 6*B*). Taken together, these results indicate (i) increased oxidation of lactate in skeletal muscle of P0 but not P1 *Oxct1*$^{-/-}$ mice and (ii) adaptation of both neonatal brain and skeletal muscle to ketolytic insufficiency.

DISCUSSION

Introduction to the extrauterine environment creates new metabolic and energetic demands. Studies of metabolic flux and ketone turnover have indicated that ketone bodies serve an important role in neonatal rodents and humans (1–3, 9, 37, 38). This is the first study to use a genetic model to demonstrate that oxidation of ketones is required for postnatal survival in mice. *Oxct1*$^{-/-}$ mice exhibit no evidence of terminal ketone body oxidation and develop ketoacidosis, indicating that the SCOT pathway is required for ketolysis in mice. Furthermore, plasma glucose and lactate levels become depleted in *Oxct1*$^{-/-}$ mice after the first 24 h of extrauterine life. Increased oxidation of glucose and lactate is observed, starting prior to the depletion of these metabolites in plasma, suggesting that increased consumption, at least in part, contributes to their depletion.

Although reduced nutrient ingestion could also contribute to ketoacidosis, hypoglycemia, and hypolactatemia, our results, together with those of prior investigators, strongly suggest that these abnormalities occur in actively suckling neonatal *Oxct1*$^{-/-}$ mice. First, because mice and rats (unlike humans) possess very little white adipose stores at birth, neonatal ketogenesis, robust in *Oxct1*$^{-/-}$ mice, is dependent on suckling (37, 38, 48). Second, plasma free fatty acid concentration, a reporter of milk intake and a key determinant of ketogenesis, exhibited

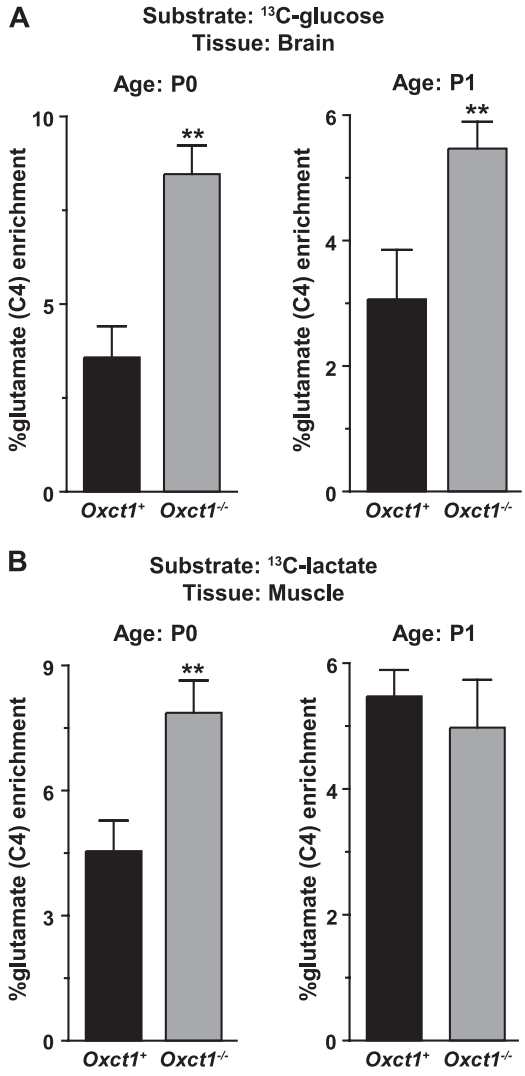

FIGURE 6. **Tissue-specific adaptations to ketolytic insufficiency.** *A*, accumulation of [^{13}C]glutamate carbon 4 (*C4*) in brains of P0 (*left*) and P1 (*right*) mice injected with [1-^{13}C]glucose, measured by ^{13}C-edited proton NMR. $n = 7$/group. *B*, accumulation of [^{13}C]glutamate in skeletal muscle of P0 (*left*) and P1 (*right*) mice injected with [3-^{13}C]lactate, measured by ^{13}C-edited proton NMR. $n = 5$/group; **, $p < 0.01$ by Student's *t* test.

increases in P1 *versus* P0 *Oxct1*$^{-/-}$ mice, comparable with the increase observed in *Oxct1*$^{+}$ littermates. Plasma triglyceride concentrations were also not reduced in *Oxct1*$^{-/-}$ mice. Although ingested milk volumes were not formally quantified, *Oxct1*$^{-/-}$ mice exhibited gastric milk spots with equal frequency to their littermates on P0 and P1. Thus, these studies indicate that loss of ketone oxidation in postnatal mice provokes a metabolic state that ultimately proves lethal, despite access to metabolic fuels through milk.

Reduced plasma glucose and lactate concentrations in P1 *Oxct1*$^{-/-}$ mice are prospectively explained by increased oxidation of glucose and lactate, but hypoglycemia and hypolactatemia also may occur due to insufficient biosynthesis. During the rodent suckling period, biosynthesis of glucose and lactate are driven by hepatic gluconeogenesis and extrahepatic glycolysis, respectively (3). Altered mitochondrial redox potential of *Oxct1*$^{-/-}$ mice could contribute to prospective synthetic deficiencies. In neonatal *Oxct1*$^{+}$ mice, plasma βOHB:AcAc ratio is 3:1, consistent with reported ratios in ketotic states (11, 39). In hyperketonemic *Oxct1*$^{-/-}$ mice, this ratio is markedly reduced to 1:2 on P0, due to oxidation of βOHB to, and no further than, AcAc, which significantly alters mitochondrial [NAD^+]:[NADH] ratio, particularly in extrahepatic tissues. Altered mitochondrial redox potential could in turn impair flux through the malate-aspartate shuttle, whose function is important for glycolysis, the source of lactate. In turn, curtailed lactate production deprives the liver of a key gluconeogenic substrate, via the Cori cycle. Furthermore, in P1 *Oxct1*$^{-/-}$ mice, plasma concentrations of βOHB and AcAc accumulate to very high concentrations, while remaining in a ratio of 1:3, which may evoke extrahepatic and hepatic impairments of the tricarboxylic acid cycle and fatty acid oxidation. Oxidative impairment within liver disrupts gluconeogenesis (3, 49–51). Emergence of attenuated extrahepatic oxidative capacity was evident in *Oxct1*$^{-/-}$ mice on P1, when glucose oxidation in brain and lactate oxidation in skeletal muscle were both reduced in *Oxct1*$^{-/-}$ mice, relative to P0 *Oxct1*$^{-/-}$ mice.

An additional abnormality of ketone metabolism may also occur in *Oxct1*$^{-/-}$ mice. In humans, up to 37% of AcAc is spontaneously decarboxylated to acetone (52). Therefore, with accumulation of high concentrations of AcAc, it is likely that acetone also accumulates in normally ketolytic tissues of *Oxct1*$^{-/-}$ mice, a notion supported by our NMR findings. Acetone is disposed through breath and urine, but a significant proportion of acetone can also be used as a substrate for anabolic and catabolic processes through SCOT-independent pathways (52). High circulating concentrations of acetone may also cause central nervous system depression.

It is important to note that the precise roles of neonatal ketone metabolism differ between mice and humans. Humans are born at a more mature point in development, and as indicated above, at the time of birth, body fat percentage is higher in humans than in rats and mice (37, 48, 53–55). In these neonatal rodents, ketogenesis is driven by suckling, rather than fasting (37, 38). Moreover, due to increased fat/carbohydrate ratio, rodent milk is more ketogenic than most human milk and infant formulas (3, 16). It is likely for these reasons that two features of *Oxct1*$^{-/-}$ mice are distinct from those of SCOT-deficient humans: (i) autosomal recessive *OXCT1* mutations in humans are compatible with life (albeit with aggressive nutritional support), whereas analysis of >100 litters of *Oxct1*$^{+/-}\times$ *Oxct1*$^{+/-}$ pairings has yet to reveal any male or female *Oxct1*$^{-/-}$ neonate that spontaneously survives past 48 h of extrauterine life; and (ii) *Oxct1*$^{-/-}$ mice develop hypoglycemia, unlike most SCOT-deficient humans. Despite these differences, deficiencies of ketone metabolism in neonatal mice bear significant relevance to human infant metabolism. First, physiological ketosis (1–2 mM) occurs in the early neonatal period in both humans and mice (1, 2, 11, 56, 57). Second, human infants are particularly prone to develop hyperketonemia and thus, increased energetic utilization of ketones, in response to relatively short periods of nutrient deprivation, due to adipose lipolysis (3, 9, 11, 14, 58). Consequences of common viral illnesses can rapidly trigger ketosis. Third, human milk exhibits significant variations of macronutrient content distribution, even within the same mother over different collections (59, 60).

Therefore, it is plausible that energetic crisis and/or ketoacidosis could emerge in infants with unsuspected ketolytic insufficiency. Current newborn screening regimens do not detect individuals with isolated ketolytic disorders, who exhibit ketosis but normal acylcarnitine and organic acid profiles (61). Therefore, a small subset of cases which ultimately receive a diagnosis of sudden infant death syndrome (SIDS) may actually be attributable to SCOT deficiency.

Although our studies did not directly measure prospective changes in glycolytic flux or metabolic shifts within myocardium (the particularly low mass of neonatal mouse heart, ~10 mg, prevented tractable NMR approaches), these results indicate both toxic effects of and metabolic adaptation to ketolytic insufficiency in the neonatal period. Future experiments will determine definitively the relative contributions of ketoacidosis, hypoglycemia, and energy deficiency to lethality of *Oxct1*$^{-/-}$ mice. Further measurement of the energetic roles of ketone bodies in mouse models will be best supported through studies in which (i) a lower fat nonketogenic nutrient formula replaces mother's milk in the neonatal period and/or (ii) additional genetic approaches selectively induce a ketolytic defect within individual tissues. Such studies will ultimately permit determination of energetic and disease-modifying roles of ketolysis in neonates and adults in conditions that include nutrient deprivation, maintenance on low carbohydrate diets, and diabetes. Finally, with increasing utilization of low and very low carbohydrate diets in clinical trials for conditions including adult obesity, pediatric and adult epilepsy, and malignancies of the central nervous system, it is important to consider the metabolic and clinical consequences of latent ketolytic defects that are revealed later in life, possibly caused by single nucleotide polymorphisms within the *OXCT1* locus; case reports describe marked variations of tolerance to ketogenic milieus (62–64). These studies indicate the critical metabolic role that ketone body oxidation serves and adaptations to its absence in the reduced carbohydrate nutrient environment of the neonatal period.

Acknowledgments—We thank Jeffrey Milbrandt, Clay Semenkovich, Rebecca Schugar, Abhinav Diwan, and Joseph Ackerman for helpful advice, and Laura Kyro for assistance with graphics.

REFERENCES

1. Ward Platt, M., and Deshpande, S. (2005) *Semin. Fetal Neonatal Med.* **10,** 341–350
2. Hawdon, J. M., Ward Platt, M. P., and Aynsley-Green, A. (1992) *Arch. Dis. Child.* **67,** 357–365
3. Girard, J., Ferré, P., Pégorier, J. P., and Duée, P. H. (1992) *Physiol. Rev.* **72,** 507–562
4. Alaynick, W. A., Kondo, R. P., Xie, W., He, W., Dufour, C. R., Downes, M., Jonker, J. W., Giles, W., Naviaux, R. K., Giguère, V., and Evans, R. M. (2007) *Cell Metab.* **6,** 13–24
5. Denne, S. C., and Kalhan, S. C. (1986) *Am. J. Physiol. Endocrinol. Metab.* **251,** E71–E77
6. Edmond, J., Robbins, R. A., Bergstrom, J. D., Cole, R. A., and de Vellis, J. (1987) *J. Neurosci. Res.* **18,** 551–561
7. Yang, S. Y., He, X. Y., and Schulz, H. (1987) *J. Biol. Chem.* **262,** 13027–13032
8. Hertz, L., and Dienel, G. A. (2002) *Int. Rev. Neurobiol.* **51,** 1–102
9. Bougneres, P. F., Lemmel, C., Ferré, P., and Bier, D. M. (1986) *J. Clin. Invest.* **77,** 42–48
10. Afifi, A. K., and Bergman, R. A. (2005) *Functional Neuroanatomy: Text and Atlas* (Afifi, A. K., and Bergman, R. A., eds) Second Ed., pp. 326–336, McGraw-Hill Company, New York
11. Cahill, G. F., Jr. (2006) *Annu. Rev. Nutr.* **26,** 1–22
12. Fukao, T., Lopaschuk, G. D., and Mitchell, G. A. (2004) *Prostaglandins Leukot. Essent. Fatty Acids* **70,** 243–251
13. Owen, O. E., Morgan, A. P., Kemp, H. G., Sullivan, J. M., Herrera, M. G., and Cahill, G. F., Jr. (1967) *J. Clin. Invest.* **46,** 1589–1595
14. Robinson, A. M., and Williamson, D. H. (1980) *Physiol. Rev.* **60,** 143–187
15. Nehlig, A. (1999) *Epilepsy Res.* **37,** 211–221
16. Morris, A. A. (2005) *J. Inherit. Metab. Dis.* **28,** 109–121
17. Sato, K., Kashiwaya, Y., Keon, C. A., Tsuchiya, N., King, M. T., Radda, G. K., Chance, B., Clarke, K., and Veech, R. L. (1995) *FASEB J.* **9,** 651–658
18. Veech, R. L. (2004) *Prostaglandins Leukot. Essent. Fatty Acids* **70,** 309–319
19. McGarry, J. D., and Foster, D. W. (1980) *Annu. Rev. Biochem.* **49,** 395–420
20. Quant, P. A., Robin, D., Robin, P., Girard, J., and Brand, M. D. (1993) *Biochim. Biophys. Acta* **1156,** 135–143
21. Quant, P. A., Robin, D., Robin, P., Girard, J., and Brand, M. D. (1989) *Biochem. Soc. Trans.* **17,** 1089–1090
22. Quant, P. A., Robin, D., Robin, P., Ferre, P., Brand, M. D., and Girard, J. (1991) *Eur. J. Biochem./FEBS* **195,** 449–454
23. Orii, K. E., Fukao, T., Song, X. Q., Mitchell, G. A., and Kondo, N. (2008) *Tohoku J. Exp. Med.* **215,** 227–236
24. Tildon, J. T., and Cornblath, M. (1972) *J. Clin. Invest.* **51,** 493–498
25. Saudubray, J. M., Specola, N., Middleton, B., Lombes, A., Bonnefont, J. P., Jakobs, C., Vassault, A., Charpentier, C., and Day, R. (1987) *Enzyme* **38,** 80–90
26. Kassovska-Bratinova, S., Fukao, T., Song, X. Q., Duncan, A. M., Chen, H. S., Robert, M. F., Pérez-Cerdá, C., Ugarte, M., Chartrand, C., Vobecky, S., Kondo, N., and Mitchell, G. A. (1996) *Am. J. Hum. Genet.* **59,** 519–528
27. Fukao, T., Mitchell, G. A., Song, X. Q., Nakamura, H., Kassovska-Bratinova, S., Orii, K. E., Wraith, J. E., Besley, G., Wanders, R. J., Niezen-Koning, K. E., Berry, G. T., Palmieri, M., and Kondo, N. (2000) *Genomics* **68,** 144–151
28. Berry, G. T., Fukao, T., Mitchell, G. A., Mazur, A., Ciafre, M., Gibson, J., Kondo, N., and Palmieri, M. J. (2001) *J. Inherit. Metab. Dis.* **24,** 587–595
29. Longo, N., Fukao, T., Singh, R., Pasquali, M., Barrios, R. G., Kondo, N., and Gibson, K. M. (2004) *J. Inherit. Metab. Dis.* **27,** 691–692
30. Fukao, T., Sakurai, S., Rolland, M. O., Zabot, M. T., Schulze, A., Yamada, K., and Kondo, N. (2006) *Mol. Genet. Metab.* **89,** 280–282
31. Kayer, M. A. (2006) *Mol. Genet. Metab.* **87,** 281–283
32. Bateman, K. S., Brownie, E. R., Wolodko, W. T., and Fraser, M. E. (2002) *Biochemistry* **41,** 14455–14462
33. Tammam, S. D., Rochet, J. C., and Fraser, M. E. (2007) *Biochemistry* **46,** 10852–10863
34. Wentz, A. E., d'Avignon, D. A., Weber, M. L., Cotter, D. G., Doherty, J. M., Kerns, R., Nagarajan, R., Reddy, N., Sambandam, N., and Crawford, P. A. (2010) *J. Biol. Chem.* **285,** 24447–24456
35. Crawford, P. A., Crowley, J. R., Sambandam, N., Muegge, B. D., Costello, E. K., Hamady, M., Knight, R., and Gordon, J. I. (2009) *Proc. Natl. Acad. Sci. U.S.A.* **106,** 11276–11281
36. Jones, J. G., Hansen, J., Sherry, A. D., Malloy, C. R., and Victor, R. G. (1997) *Anal. Biochem.* **249,** 201–206
37. Girard, J. R., Cuendet, G. S., Marliss, E. B., Kervran, A., Rieutort, M., and Assan, R. (1973) *J. Clin. Invest.* **52,** 3190–3200
38. Ferré, P., Pégorier, J. P., Williamson, D. H., and Girard, J. R. (1978) *Biochem. J.* **176,** 759–765
39. Cahill, G. F., Jr., Herrera, M. G., Morgan, A. P., Soeldner, J. S., Steinke, J., Levy, P. L., Reichard, G. A., Jr., and Kipnis, D. M. (1966) *J. Clin. Invest.* **45,** 1751–1769
40. Soeters, M. R., Sauerwein, H. P., Faas, L., Smeenge, M., Duran, M., Wanders, R. J., Ruiter, A. F., Ackermans, M. T., Fliers, E., Houten, S. M., and Serlie, M. J. (2009) *Obesity* **17,** 1326–1331
41. MacDonald, M. J., Longacre, M. J., Stoker, S. W., Brown, L. J., Hasan, N. M., and Kendrick, M. A. (2008) *Am. J. Physiol. Cell Physiol.* **294,** C442–C450
42. Hasan, N. M., Longacre, M. J., Seed-Ahmed, M., Kendrick, M. A., Gu, H.,

Ostenson, C. G., Fukao, T., and MacDonald, M. J. (2010) *Arch. Biochem. Biophys.* **499,** 62–68
43. Matsui, Y., Takagi, H., Qu, X., Abdellatif, M., Sakoda, H., Asano, T., Levine, B., and Sadoshima, J. (2007) *Circ. Res.* **100,** 914–922
44. Glick, D., Barth, S., and Macleod, K. F. (2010) *J. Pathol.* **221,** 3–12
45. Yu, L., McPhee, C. K., Zheng, L., Mardones, G. A., Rong, Y., Peng, J., Mi, N., Zhao, Y., Liu, Z., Wan, F., Hailey, D. W., Oorschot, V., Klumperman, J., Baehrecke, E. H., and Lenardo, M. J. (2010) *Nature* **465,** 942–946
46. Kuma, A., Hatano, M., Matsui, M., Yamamoto, A., Nakaya, H., Yoshimori, T., Ohsumi, Y., Tokuhisa, T., and Mizushima, N. (2004) *Nature* **432,** 1032–1036
47. Barth, S., Glick, D., and Macleod, K. F. (2010) *J. Pathol.* **221,** 117–124
48. Barnett, S. A., and Widdowson, E. M. (1971) *J. Reprod. Fertil.* **26,** 39–57
49. Krebs, H. A. (1967) *Natl. Cancer Inst. Monogr.* **27,** 331–343
50. Takahashi, M., Ueda, K., Tabata, R., Iwata, S., Ozawa, K., Uno, S., and Kinoshita, M. (1997) *J. Lab. Clin. Med.* **129,** 72–80
51. Burgess, S. C., Leone, T. C., Wende, A. R., Croce, M. A., Chen, Z., Sherry, A. D., Malloy, C. R., and Finck, B. N. (2006) *J. Biol. Chem.* **281,** 19000–19008
52. Reichard, G. A., Jr., Haff, A. C., Skutches, C. L., Paul, P., Holroyde, C. P., and Owen, O. E. (1979) *J. Clin. Invest.* **63,** 619–626
53. Hagberg, H., Peebles, D., and Mallard, C. (2002) *Mental Retard. Dev. Disabilities Res. Rev.* **8,** 30–38
54. Hew, K. W., and Keller, K. A. (2003) *Birth Defects Res.* **68,** 309–320
55. Ibáñez, L., Sebastiani, G., Lopez-Bermejo, A., Díaz, M., Gómez-Roig, M. D., and de Zegher, F. (2008) *J. Clin. Endocrinol. Metab.* **93,** 2774–2778
56. McGarry, J. D., and Foster, D. W. (1977) *Arch. Int. Med.* **137,** 495–501
57. Hondares, E., Rosell, M., Gonzalez, F. J., Giralt, M., Iglesias, R., and Villarroya, F. (2010) *Cell Metab.* **11,** 206–212
58. Chaussain, J. L., Georges, P., Calzada, L., and Job, J. C. (1977) *J. Pediatr.* **91,** 711–714
59. Jenness, R. (1979) *Semin. Perinatol.* **3,** 225–239
60. Allen, J. C., Keller, R. P., Archer, P., and Neville, M. C. (1991) *Am. J. Clin. Nutr.* **54,** 69–80
61. Mitchell, G. A., and Fukao, T. (2000) in *The Online Metabolic and Molecular Bases of Inherited Diseases (OMMBID)* (Beaudet, A., Vogelstein, B., Kinzler, K. W., Antonarakis, S., and Ballabio, A., eds), McGraw-Hill Book Company, Columbus, OH
62. Best, T. H., Franz, D. N., Gilbert, D. L., Nelson, D. P., and Epstein, M. R. (2000) *Neurology* **54,** 2328–2330
63. Chen, T. Y., Smith, W., Rosenstock, J. L., and Lessnau, K. D. (2006) *Lancet* **367,** 958
64. Owen, D., Little, S., Leach, R., and Wyncoll, D. (2008) *Intensive Care Med.* **34,** 971–972